IEEE Access
Multidisciplinary | Rapid Review | Open Access Journal

Received March 22, 2020, accepted April 9, 2020, date of publication April 22, 2020, date of current version June 3, 2020.

Digital Object Identifier 10.1109/ACCESS.2020.2989503

Successive Decode-and-Forward Relaying With Privacy-Aware Interference Suppression

JIANJING WEI[1], JIE WEI[1], SHAOLING HU[2], (Graduate Student Member, IEEE), AND WEI CHEN[2], (Senior Member, IEEE)

[1]School of Electronic and Information Engineering, Beijing Jiaotong University, Beijing 100044, China
[2]Department of Electronic Engineering, Tsinghua University, Beijing 100084, China

Corresponding author: Jie Wei (jwei@bjtu.edu.cn)

This work was supported in part by the Beijing Natural Science Foundation under Grant 4191001, in part by the National Science Foundation of China under Grant 61971264, and in part by the National key research and development program 2018YFA0701601.

ABSTRACT Successive relaying holds the promise of achieving spatial diversity gain for single-antenna users while recovering the multiplexing loss due to the half-duplex relaying in B5G/6G. However, how to mitigate inter-relay interference (IRI) with privacy protection in low complexity remains open. In this paper, we present a successive decode-and-forward (DF) relaying protocol based on an analog network interference cancellation (NICE) method, which may suppress IRI, using linear processing without decoding the signals from the source. More specifically, a relay actively keeps receiving signals from the source, which are then used as prior knowledge to enable an amplify-and-cancel (AC) IRI mitigation strategy. The AC based IRI suppression is capable of improving high information privacy, because a relay does not need to know codebooks used by other relays and will not decode any signals intended for other relays. We obtain the closed-form expression of the minimum residual interference power, based on which the average throughput and the optimal diversity-multiplexing tradeoff (DMT) are presented. The DMT analysis along with simulations shows that the proposed method outperforms conventional two-timeslot half-duplex relaying in terms of the spectral efficiency. It also achieves lower complexity than CAO-SIR based on decode-and-cancel (DC) in [1] and lower IRI than the successive amplify-and-forward (AF) relaying in [2].

INDEX TERMS Cooperative diversity, successive relaying, inter-relay interference, decode-and-forward, interference suppression, power allocation, diversity multiplexing tradeoff.

I. INTRODUCTION

With the initial deployment of 5G network all around the world, efforts from academia and industry start to look beyond 5G and start the research of B5G/6G [3], [4]. B5G/6G will require higher data rates and denser connection for supporting Artificial Intelligence (AI) services and Internet of Everything (IoE). Cooperative communication is a potential technology to achieve these goals with low-cost equipment and low implementation complexity, by providing spatial diversity and extending the coverage.

Cooperative communication was first proposed for a conventional CDMA system in [5] and [6]. From then on, there have been many research on cooperative communication. The space diversity and DMT of various cooperative relaying schemes including fixed relaying, selection relaying, and incremental relaying were studied in [7] and [8]. It was shown that most of the proposed protocols achieve full diversity. The spatial diversity gains of three different cooperative protocols were discussed over fading channels [9]. It was shown that the protocols that employ the appropriate power control can achieve full spatial diversity. The opportunistic relaying protocol based on network path selection was proposed in [10], where only one best relay will be selected and used for cooperation between the source and the destination. Most of the cooperative diversity protocols mentioned above are two-timeslot relaying protocols, in which relays receive signals from the source in the first timeslot and forward their signals to the destination in the second timeslot. However, these two-timeslot relaying protocols have to suffer severe multiplexing loss due to the half-duplex constraint of relays. The multiplexing gains in these two-timeslot relaying protocols are

The associate editor coordinating the review of this manuscript and approving it for publication was Celimuge Wu.

upper bounded by 1/2. To overcome this severe multiplexing loss, the cooperative relaying networks using full-duplex relays were studied in recent works [11], [12], in which relays transmit and receive signals simultaneously. However, the self-interference is caused at the full-duplex relays, which makes the implementation of the full-duplex relaying quite demanding in practice.

Instead of using full-duplex relays, successive relaying is an alternative method to recover severe multiplexing loss, the basic idea of which relies on the concurrent transmission of the source and the relays [13], [14]. More specifically, the source transmits its signal to one relay, while another relay transmits its signal to the destination simultaneously. Therefore, successive relaying with half-duplex relays can approach the full-duplex mode when a large number of relays are employed to participate in cooperative transmission. It is also referred to as ''Virtual Full-Duplex Relaying''. However, the concurrent transmission of the source and the relays may cause severe inter-relay interference (IRI), thereby decreasing the transmission rate. Therefore, the suppression of IRI becomes a critical issue for successive relaying. At present, many interference cancellation schemes have been designed to cancel or mitigate the IRI in successive relaying.

For amplify-and-forward (AF)-based successive relaying, various IRI cancellation methods have been proposed in [15]– [19]. An inter-relay self-interference cancellation method was investigated to cancel the IRI at relay nodes for AF-based two-path successive relaying protocol [15]. Full interference cancellation (FIC) and partial interference cancellation (PIC) were proposed to suppress the IRI at the destination for the two-path successive relaying systems in [16] and [17]. More recently, a precoding-based interference cancellation scheme based on row-space mapping was proposed for AF two-path successive relay networks [18], where a combined decoding and re-encoding scheme is designed to cancel the IRI signal and the accumulated noise at relays without any knowledge of channel state information (CSI). A successive two-way relaying system that uses two half-duplex relays was studied to mimic the full-duplex two-way relaying in [19], where the IRI can be mitigated by using a generalized self-interference (GSI) mitigation method.

For decode-and-forward (DF)-based successive relaying, lots of IRI cancellation methods have been proposed in [20]- [23]. Zhang applied the ''dirty-paper-coding (DPC)'' technique into DF-based successive relaying to mitigate the IRI at source transmitter [20]. Successive interference cancellation (SIC) at the relays was proposed to improve the performance of diversity multiplexing tradeoff (DMT) in DF-based two-path half-duplex relaying [21]. An IRI mitigation scheme under a capacity constraint was employed to cancel the effect of IRI in DF-based two-path successive relaying [22]. In [23], an interference mitigation method using relay selection and joint decoding was adopted to achieve full diversity gain and high multiplexing gain in multiple-relay cooperative networks. The work [24] investigated an energy harvesting (EH) based DF two-path half-duplex relaying network, in which power splitting ratio between EH and information decoding (ID) is optimized to mitigate IRI.

In this regard, we present Network Interference CancEllation (NICE) as an efficient interference cancellation method in our previous work [25]. More specifically, an interfered node can obtain the prior knowledge about the interference by actively listening to the source. The prior knowledge can be used to mitigate the interference. Even though the relay nodes can receive the signals from the source and the other relay nodes, if the relay nodes are malicious, but not granted, it is not easy for them to crack the information [26]- [29]. In [25], we developed two NICE protocols, namely, amplify-and-cancel (AC) and decode-and-cancel (DC). The AC method means that an interfered node can mitigate the interference with analog signal processing. The DC method enables the interfered nodes to decode the prior received signals. Furthermore, we presented a DF-based successive relaying protocol, also referred to as CAO-SIR scheme, where the DC protocol is extended to completely cancel the IRI [1]. However, there may be decoding error and error propagation in this work, while privacy disclosure may be caused due to that a relay is allowed to decode the signals intended for other relays. Recently, we have extended the AC protocol to mitigate the IRI in AF-based successive relaying [2], which avoids privacy disclosure and achieves low complexity. However, the noise and residual interference are amplified along with the desired signal at AF relays, which may result in poor transmission rate.

In this paper, we investigate a successive relaying protocol, in which an analog signal processing is used to suppress IRI at each relay node. Specifically, a relay actively keeps listening for signals from the source. The prior received signals are given different weights to mitigate IRI at relay nodes. After IRI suppression, relays decode the desired signals from the processed signals and then forward the signals to the destination. We obtain the optimal weights that minimize the residual interference power at relay nodes. We further give the closed-form expression of the minimum residual interference power. It is shown that the minimum power of residual interference is bounded even if the transmission power approaches infinity. Based on the boundedness of minimum residual interference power, we present the average throughput and the DMT performance of our scheme. Furthermore, to improve power efficiency, we study the power allocation scheme in the high SNR regime for this successive relaying protocol. In contrast to our previous work [1], we avoid decoding the interference signals that are desired signals for other relays, thus ensuring the information privacy. Compared to our previous work [2], relay nodes decode and forward the desired signals to node D in our scheme, which reduces the interference and increases the transmission rate.

The rest of this paper is organized as follows. Section II presents the system model. A successive decode-and-forward relaying with privacy-aware low-complexity interference suppression is presented in Section III. Section IV analyzes the power of residual interference, average throughput and

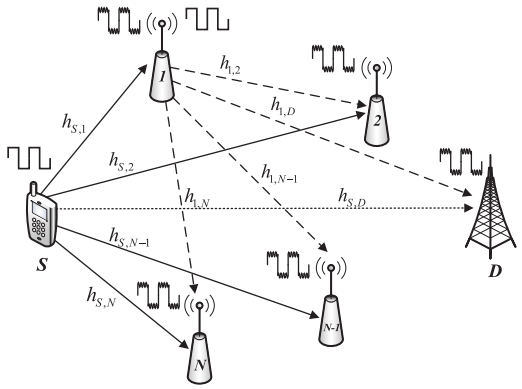

FIGURE 1. System model.

DMT performance of our scheme. We also investigate the power allocation scheme in the high SNR regime for the proposed protocol in Section IV. Finally, the numerical results and conclusion are presented in Section V and Section VI, respectively.

II. SYSTEM MODEL

We consider a cooperative communication system, consisting of one source node S, one destination node D, and N relay nodes, as shown in Fig. 1. The set of relay nodes is denoted by $\{1, 2, \ldots, N\}$. All the relays work in the half-duplex and decode-and-forward mode. We consider a slow fading and independent quasi-static channel model. Assume that the channel state remains constant in each successive relaying period. We use $h_{a,b}$ to denote the channel coefficient of the link between nodes a and b, $a \in \{S, 1, \ldots, N\}$ and $b \in \{1, \ldots, N, D\}$. Let $g_{a,b}$ denote the channel gain of the link between nodes a and b, namely, $g_{a,b} = |h_{a,b}|^2$.

To obtain the channel coefficients of all links, we adopt channel estimation with a pilot and Channel State Information (CSI) feedback. The same method has been used in lots of works on the cooperative communication [1], [34], [35]. More specifically, the source node and the relay nodes first broadcast the pilots at the beginning of each successive relaying period. A relay can receive the broadcast pilots and then estimate the channel coefficients of links spanning from the source node and other relay nodes to itself accordingly. The destination node can estimate the channel coefficients of the source-destination and relay-destination links. As a result, the relay nodes and the destination node obtain the CSI of the source-relay, source-destination, relay-relay, and relay-destination channels. Finally, the CSI of all links is fed back to the source via signaling channels.

Throughout this paper, time-slotted scheduling is assumed. Let $X_a[k]$ denote the signal transmitted by node a in the kth timeslot. We use $Y_b[k]$ to denote the received signal in the kth timeslot at node b. Due to the half-duplex constraint of the relays, we have $b \neq a$. The received signal $Y_b[k]$ can be obtained by

$$Y_b[k] = \sum_{a \in \mathcal{T}[k]} h_{a,b} X_a[k] + Z_b[k], \tag{1}$$

in which $\mathcal{T}[k]$ is the set of nodes that are transmitting in the kth timeslot. Notation $Z_b[k]$ denotes the Additive White Gaussian Noise (AWGN) at node b and subjects to normal distribution with zero mean and a variance of σ^2, i.e., $Z_b[k] \sim \mathcal{CN}(0, \sigma^2)$.

III. SUCCESSIVE DECODE-AND-FORWARD RELAYING PROTOCOL WITH INTERFERENCE SUPPRESSION

In this section, we first introduce the scheduling process of this successive relaying protocol. Since the concurrent transmission of the source node and the relay nodes will cause severe interference at the receiving nodes in this protocol, we next focus on the interference suppression schemes at the relay nodes and the destination node, respectively.

The entire transmission process costs $(N + 1)$ timeslots when N relays are employed in this successive relaying, as shown in Fig. 2. In the first timeslot, only node S broadcasts its first symbol to the relay nodes and the destination node D. In the following nth timeslot, $n = 2, 3, \ldots, N$, node S continues to broadcast its nth symbol to relay nodes and node D, while the $(n-1)$th relay node forwards its decoded messages to node D concurrently. The relay nodes that have not yet forwarded their signals to the destination are all required to overhear the source node. In the $(N+1)$ timeslot, only relay node N transmits to node D. The above scheduling strategy yields the following equivalent baseband signal model. At relay node, the received signals are given by

$$Y_n[1] = h_{S,n} X_S[1] + Z_n[1], \tag{2}$$

$$Y_n[k] = h_{S,n} X_S[k] + h_{k-1,n} X_{k-1}[k] + Z_n[k], \quad k = 2, \ldots, n. \tag{3}$$

At node D, the received signals are given by

$$Y_D[1] = h_{S,D} X_S[1] + Z_D[1], \tag{4}$$

$$Y_D[n] = h_{S,D} X_S[n] + h_{n-1,D} X_{n-1}[n] + Z_D[n], \quad n = 2, \ldots, N, \tag{5}$$

$$Y_D[N+1] = h_{N,D} X_N[N+1] + Z_D[N+1]. \tag{6}$$

In Eqs. (3) and (5), notation $X_n[n+1]$ is the transmitted signal at relay node n that acquires $X_n[n+1]$ from its received signal $Y_n[n]$. To obtain this $X_n[n+1]$, an IRI suppression scheme should be executed first by the relay node n. In this IRI suppression scheme, relay node n first keeps in buffer the signals received from the first timeslot to the $(n-1)$th timeslot, which will be used as the prior knowledge of the IRI. To buffer the received signals, the analog signals are quantized to digital signals. This conversion brings in additional quantization noise that may degrade the performance of the network. However, with enough resolution, the quantization noise can be ignored [30], [31]. Next, these previously received signals are subtracted from $Y_n[n]$ with different weights. As shown

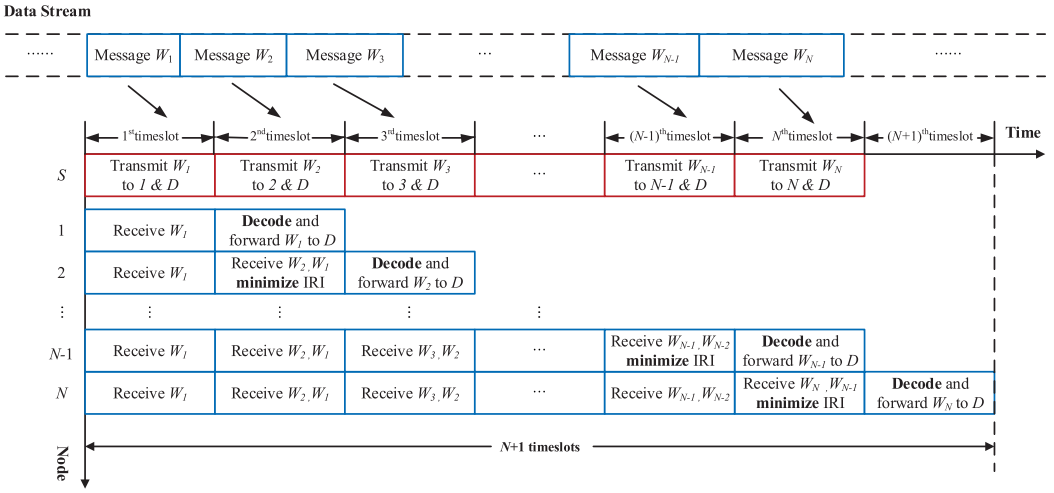

FIGURE 2. Time-slotted scheduling strategy.

in Fig. 4, we use $\omega_n[j]$ to denote the weight for $Y_n[j]$. After this IRI suppression, the processed signal Y_n^{AC} at relay node n is given by

$$Y_n^{AC} = Y_n[n] - \sum_{j=1}^{n-1} \omega_n[j] Y_n[j]. \tag{7}$$

Then, this signal Y_n^{AC} is decoded and forwarded by relay node n. Relay node will empty its buffer after finishing its transmission to node D. The signal processing at relay node n is specifically presented in Algorithm 1.

Algorithm 1 The Signal Processing at Relay Node n

Input: $\boldsymbol{\omega}_n$,
(Relay node n gets $\boldsymbol{\omega}_n$ from node S through signaling channel)

Output: $X_n[n+1]$.

for $i = 1 : n$ **do**
  Receive and cache the signal $Y_n[i]$.
  if $i = n$ **then**
    Suppress the interference from relay node $(n-1)$ by Eq. (7).
    Get $X_S[n]$ by decoding signal Y_n^{AC} in Eq. (7).
    Construct $X_n[n+1]$ by re-encoding $X_S[n]$.
  end if
end for
return $X_n[n+1]$.

In this protocol, the same modulation and coding scheme is applied at the source and relay node when they transmit the same signals. Since different signals are retransmitted, the modulation and coding schemes are varied at different relay nodes. Rate adaptation is used to ensure that the decoding at relay nodes is error-free. Furthermore, it is assumed that the same transmission power is used at all nodes, which is consistent with the settings in [7], [8], [10], [14], [32]. As a result, we naturally obtain

$$X_n[n+1] = X_S[n]. \tag{8}$$

It is important to note that the IRI suppression scheme in this protocol is distinctly different from the interference suppression schemes in our previous works [1] and [2]. We list the main differences of these IRI suppression schemes in Fig. 3. More specifically, in [1], relay nodes should be carefully ordered to ensure that the interference signals can be completely decoded at each relay node. Therefore, the interference signals are thoroughly canceled before the desired signals are decoded at relay nodes. Since all the previously received signals should be decoded at relay nodes, the protocol in [1] has a high risk of privacy disclosure and error propagation. In [2], relay nodes have no need to decode any previously received signals. The IRI suppression scheme is executed with the received analog signals and the desired signal is amplified and forwarded to node D by relay node. As a result, the protocol in [2] has an advantage of low complexity and information privacy. Due to the analog signal processing, the interference cannot be canceled thoroughly, which causes a significant decrease in transmission rate for the protocol in [2]. In this work, the IRI suppression scheme shares the benefits of the schemes in [1] and [2], while avoids their disadvantages simultaneously. In more detail, the previously received signals are not decoded at relay nodes, which avoids the privacy disclosure. Due to the analog signal processing, the IRI suppression scheme in this work also has low complexity. Furthermore, relay nodes decode the desired signals before transmitting them to the node D, which reduces the interference to node D and increases the channel capacity.

Having presented the scheduling processing of the proposed protocol and the differences of IRI suppression scheme with our previous works, we next focus on how to obtain the optimal weights $\{\omega_n[j]\}_{j=1}^{n-1}$ for each relay node. By substituting Eq. (8) into Eq. (3), the previously received signals at

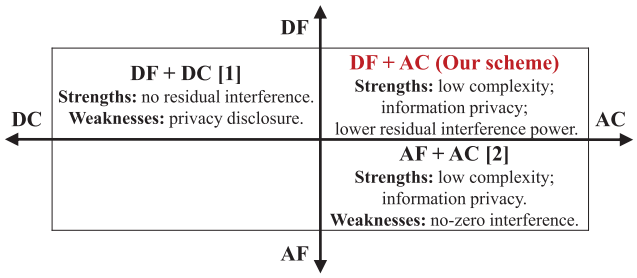

FIGURE 3. The main differences between the proposed protocol and our previous works [1] and [2].

relay node n are shown by

$$\boldsymbol{y}_n = \sum_{j=1}^{n-1} \left(\boldsymbol{\alpha}_{n,j} X_S[j] + \boldsymbol{e}_{n,j} Z_n[j]\right), \tag{9}$$

where

$$\boldsymbol{y}_n = [Y_n[1], Y_n[2], \ldots, Y_n[n-1]]^\intercal, \tag{10}$$

$$\boldsymbol{\alpha}_{n,j} = [\mathbf{0}_{1,j-1}, h_{S,n}, h_{j,n}, \mathbf{0}_{1,n-j-2}]^\intercal, \quad j=1,\ldots,n-2, \tag{11}$$

$$\boldsymbol{\alpha}_{n,n-1} = [\mathbf{0}_{1,n-2}, h_{S,n}]^\intercal, \tag{12}$$

$$\boldsymbol{e}_{n,j} = [\mathbf{0}_{1,j-1}, 1, \mathbf{0}_{1,n-j-1}]^\intercal. \tag{13}$$

In Eqs. (10)-(13), notation $\intercal$ denotes the matrix transpose and $\mathbf{0}_{1,j}$ denotes the j-dimensional row vector whose elements are all zeros. Define that $\boldsymbol{\omega}_n = [\omega_n[1], \omega_n[2], \ldots, \omega_n[n-1]]^\intercal$. From Eq. (7), the residual interference at relay node n is shown by $h_{n-1,n}X_{n-1}[n] - \boldsymbol{\omega}_n^\intercal \boldsymbol{y}_n$. Therefore, the power of residual interference is obtained by

$$I_n = \mathbb{E}\left\{\left|h_{n-1,n}X_{n-1}[n] - \boldsymbol{\omega}_n^\intercal \boldsymbol{y}_n\right|^2\right\}. \tag{14}$$

To minimize the residual interference power I_n, the optimal weight vector $\boldsymbol{\omega}_n$ is given in the following theorem.

Theorem 1: The optimal weight vector $\boldsymbol{\omega}_n$ is given by

$$\boldsymbol{\omega}_n^\intercal = h_{n-1,n}\boldsymbol{\alpha}_{n,n-1}^{\mathbf{H}} \mathbf{B}_n^{-1} P, \tag{15}$$

where

$$\mathbf{B}_n = \sum_{j=1}^{n-1} \boldsymbol{\alpha}_{n,j}\boldsymbol{\alpha}_{n,j}^{\mathbf{H}} P + \mathbf{E}_{n-1}\sigma^2. \tag{16}$$

Notation $\mathbf{H}$ denotes Hermitian transpose, while $\mathbf{E}_{n-1}$ denotes the $(n-1)$-by-$(n-1)$ identity matrix.

Proof: See Appendix A. ∎

Having presented the IRI suppression scheme at relay nodes, we next turn our attention to the interference cancellation method at node D. As shown in Eq. (5), the interference at node D is caused by the signals from node S. To cancel the interference from node S, we apply a reverse successive decoding method presented in Algorithm 2. More specifically, node D first decodes $X_S[N]$ from its last received signal $Y_D[N+1]$ in which there is no interference from node S.

Algorithm 2 Reverse Successive Decoding for D

Decode message W_N from $Y_D[N+1]$
For $k = N : -1 : 2$
Construct $X_S[k]$ by re-encoding W_k
Cancel the interference from node S by Eq. (17)
Decode message W_{k-1} from the right side of Eq. (17)
End

Then node D reconstructs the signal $h_{S,D}X_S[N]$ with local CSI $h_{S,D}$. Signal $h_{S,D}X_S[N]$ is next subtracted from $Y_D[N]$ so that the interference from direct link is canceled thoroughly. Node D can obtain $X_S[N-1]$ from the residual signal $h_{N-1,D}X_{N-1}[N] + Z_D[N]$. In this way, for $n = 1, \ldots, N-1$, node D first acquires $X_S[n+1]$ and then reconstructs the signal $h_{S,D}X_S[n+1]$. Using this signal $h_{S,D}X_S[n+1]$, node D cancels the interference from node S by

$$Y_D[n+1] - h_{S,D}X_S[n+1] = h_{n,D}X_n[n+1] + Z_D[n+1]. \tag{17}$$

Signal $X_S[n]$ can be then decoded from $h_{n,D}X_n[n+1] + Z_D[n+1]$.

IV. PERFORMANCE ANALYSIS

In this section, we first present the closed-form expression of the minimum residual interference power. It is next shown that the minimum residual interference power is bounded even if the transmission power approaches infinity. Based on the analysis of residual interference power, we then obtain the average throughput. Furthermore, diversity-multiplexing tradeoff is analyzed to show more insight of this protocol. Finally, the power allocation scheme is investigated in the high SNR regime for this protocol.

A. RESIDUAL INTERFERENCE POWER

We have given the optimal weight vector that minimizes the residual interference power in Theorem 1. The minimum power of residual interference of this successive relaying protocol is presented in the following theorem.

Theorem 2: When $\boldsymbol{\omega}_n$ in Eq. (15) is used for IRI suppression scheme at relay node n, the minimum power of residual interference is given by

$$I_n(P) = g_{n-1,n}P\left(1 - \boldsymbol{\alpha}_{n,n-1}^{\mathbf{H}}\mathbf{B}_n^{-1}(P)\boldsymbol{\alpha}_{n,n-1}P\right). \tag{18}$$

Proof: See Appendix B. ∎

Remark 1: From Theorem 2, it is seen that the minimum power of residual interference at relay node n depends on two factors. One factor is the channel state of the link from relay node $n-1$ to relay node n. When the channel state between relay node $n-1$ and relay node n is in deep fading, minor interference would be caused between these two relay nodes. The other factor is the IRI suppression scheme used at relay node n. By using the IRI suppression scheme at relay node n, the interference power is reduced by $g_{n-1,n}\boldsymbol{\alpha}_{n,n-1}^{\mathbf{H}}\mathbf{B}_n^{-1}(P)\boldsymbol{\alpha}_{n,n-1}P^2$.

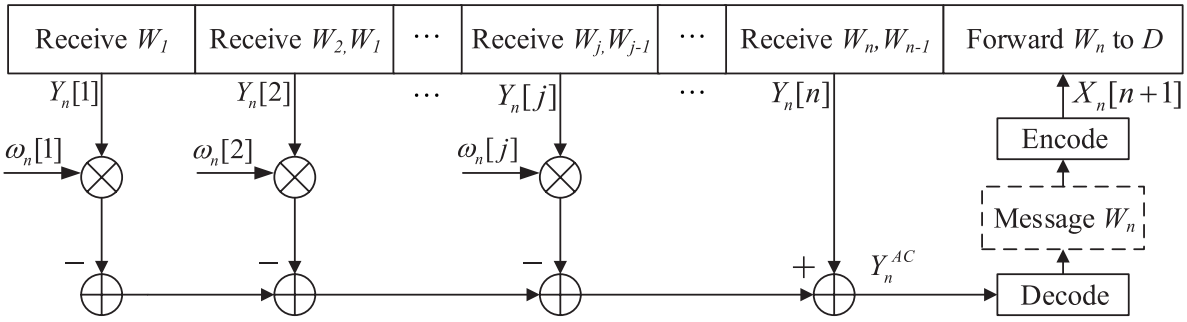

FIGURE 4. Inter-relay interference suppression method.

From Theorem 2, the minimum power of residual interference $I_n(P)$ is a function of transmission power P. In the following, we next show that $I_n(P)$ is bounded even if the transmission power P approaches infinity.

Theorem 3: The minimum power of residual interference $I_n(P)$ is asymptotically obtained in the high SNR regime by

$$\lim_{P\to\infty} I_n(P) = \sigma^2 \sum_{j=1}^{n-1} \frac{\prod_{k=j}^{n-1} g_{k,n}}{g_{S,n}^{n-j}}. \tag{19}$$

Proof: The main idea of this proof is to take the asymptotic expression of $\omega_n[j]$ in the high SNR regime into Eq. (56). From Eq. (15), we first give the expression of the weight $\omega_n[j]$ in high SNR regime by

$$\lim_{P\to\infty} \omega_n[j] = (-1)^{n-j-1} \frac{\prod_{k=j}^{n-1} h_{k,n}}{h_{S,n}^{n-j}}. \tag{20}$$

When $\omega_n[j] = (-1)^{n-j-1} \frac{\prod_{k=j}^{n-1} h_{k,n}}{h_{S,n}^{n-j}}$, then it can be observed that

$$\begin{aligned} h_{n-1,n} - \omega_n[n-1] h_{S,n} &= 0, \\ \boldsymbol{\omega}_n^{\intercal} \boldsymbol{\alpha}_{n,j} &= 0, \end{aligned} \tag{21}$$

which implies that the signals $X_S[j], j \in \{1, \ldots, n-1\}$, in Y_n^{AC} are canceled completely at relay node n by this IRI suppression scheme. As a result, we have

$$\begin{aligned} \lim_{P\to\infty} I_n(P) &= \lim_{P\to\infty} \sigma^2 \sum_{j=1}^{n-1} |\boldsymbol{\omega}_n^{\intercal} \boldsymbol{e}_{n,j}|^2 \\ &= \lim_{P\to\infty} \sigma^2 \sum_{j=1}^{n-1} \omega_n^2[j]. \end{aligned} \tag{22}$$

By substituting Eq. (20) into Eq. (22), we get Eq. (19). Thus, Theorem 3 is established. ∎

It is seen from Eq. (53) that the minimum residual interference power may be divided into two parts: one is induced by messages, the other is induced by noise. From the proof of Theorem 3, we know that the power of residual interference caused by messages approaches zero when the transmission power approaches infinity, while the power of residual interference caused by noise cannot be canceled completely. Furthermore, the minimum power of residual interference $I_n(P)$ is bounded in the high SNR regime.

B. AVERAGE THROUGHPUT

Based on the above analysis of residual interference power, we know that the IRI at relay nodes cannot be canceled thoroughly. The capacity of each source-relay link is decreased because of the residual interference. However, Theorem 3 implies that the minimum power of residual interference $I_n(P)$ is bounded even if the transmission power P approaches infinity. From the boundedness of $I_n(P)$ and Shannon's formula, we next give the average throughput of this successive relaying protocol in the following theorem.

Theorem 4: The average throughput of this successive relaying protocol is given by

$$\bar{C} = \frac{1}{N+1} \sum_{n=1}^{N} C_n, \tag{23}$$

in which C_n denotes the channel capacity of the equivalent link $S - n - D$. The channel capacity C_n is obtained by

$$C_n = \log\left(1 + \min\left\{\frac{g_{S,n}P}{I_n + \sigma^2}, \frac{g_{n,D}P}{\sigma^2}\right\}\right). \tag{24}$$

Proof: The main idea of this proof is to prove the channel capacity C_n in Eq. (24). For this purpose, we use $C_{S,n}$ and $C_{n,D}$ to denote the channel capacity of the equivalent link $S - n$ and $n - D$, respectively. Since the decode-and-forward protocol is used at relay node n, the channel capacity of the equivalent link $S - n - D$ is determined by the minimum channel capacity of the equivalent link $S - n$ and $n - D$, i.e., $C_n = \min\{C_{S,n}, C_{n,D}\}$.

We first give the channel capacity $C_{S,n}$. Based on Eqs. (3) and (7), the SINR of the processed signal at relay node n is given by

$$\gamma_n = \frac{g_{S,n}P}{I_n + \sigma^2}, \tag{25}$$

in which I_n is given by Eq. (18) in Theorem 2. Thus, the channel capacity $C_{S,n}$ is obtained by

$$C_{S,n} = \log\left(1 + \frac{g_{S,n}P}{I_n + \sigma^2}\right). \tag{26}$$

Algorithm 3 The Exhaustive Method to Obtain the Optimal Relay Ordering of N Relays

Input: $h_{a,b}$, where $a \in \{S, 1, \ldots, N\}$ and $b \in \{1, \ldots, N, D\}$, P, and σ^2.

Output: $\boldsymbol{\omega}_n^*$ and $\{(n)^*\}_{n=1}^N$.

1: $\bar{C}^* \leftarrow 0$.
2: **for** each $\{(n)\}_{n=1}^N \in \mathcal{S}$ **do**
3: Get $\boldsymbol{\omega}_n$ and I_n by Eqs. (15) and (18), respectively.
4: Calculate $\bar{C}$ with Eqs. (23) and (24).
5: **if** $\bar{C}^* < \bar{C}$ **then**
$\bar{C}^* = \bar{C}$, $\boldsymbol{\omega}_n^* = \boldsymbol{\omega}_n$, and $\{(n)^*\}_{n=1}^N = \{(n)\}_{n=1}^N$.
6: **end if**
7: **end for**
8: **return** $\boldsymbol{\omega}_n^*$ and $\{(n)^*\}_{n=1}^N$.

Given the channel capacity $C_{S,n}$, we next give the channel capacity $C_{n,D}$. From the right side of Eq. (17), the SNR of the processed signal at the node D is given by

$$\gamma_D = \frac{g_{n,D}P}{\sigma^2}. \tag{27}$$

Thus, the channel capacity $C_{n,D}$ is obtained by

$$C_{n,D} = \log\left(1 + \frac{g_{n,D}P}{\sigma^2}\right). \tag{28}$$

Based on Eqs. (26) and (28), we obtain the channel capacity C_n in Eq. (24). Since all the messages W_k, $k = 1, 2, \ldots, N$, are reliably transmitted within $N+1$ timeslots, when N relays are employed in the propose protocol. We obtain the average throughput of this successive relaying protocol given in Eq. (24), which completes the proof. ∎

Since the node S has collected the CSI of all links, the transmitter has known the capacity before transmission. Thus, the Adaptive Modulation and Coding (AMC) can be used to fully use the channel capacity. Moreover, based on Eqs. (19) and (24), the channel capacity C_n is asymptotically obtained in the high SNR regime by $\lim_{P\to\infty} C_n = \lim_{P\to\infty} \log P$. It is seen that the channel capacity C_n is an increasing function of transmission power P. Furthermore, the degree of freedom for this successive relaying protocol is given by $\lim_{P\to\infty} \frac{\bar{C}}{\log P} = \frac{N}{N+1}$.

It is noted that the minimum power of residual interference changes when different relay orderings are used. Therefore, the average throughput and the outage probability will change when relay ordering is different. To maximize the average throughput of this successive relaying, the exhaustive method is adopted to obtain the optimal relay ordering of N relays in Algorithm 3. In more detail, first, the source collects the CSI of all links by using the channel estimation with training sequence and CSI feedback. Second, based on the collected CSI, the source calculates the weight vector and the average throughput by Eqs. (15), (23) and (47) for all possible relay orderings. Finally, the source can determine the optimal relay ordering that has the maximum throughput and broadcast it back to the relays. We use $\mathcal{S}$ to denote the set of all possible relay orderings with N relays. Let $\{(n)\}_{n=1}^N$ denote one element in $\mathcal{S}$ and $\{(n)^*\}_{n=1}^N$ denote the optimal relay ordering. Notations $\boldsymbol{\omega}_n^*$ and $\bar{C}^*$ denote the weight vector and the average throughput under the optimal relay ordering, respectively.

C. DIVERSITY-MULTIPLEXING TRADEOFF

Having analyzed the residual interference power and average throughput of this successive relaying protocol, we present the outage probability and the DMT of our scheme in the following context.

Let r and $d(r)$ denote the multiplexing gain and the diversity gain that is a function of the multiplexing gain, respectively. The diversity gain $d(r)$ is defined as

$$d(r) = -\lim_{\gamma\to\infty} \frac{\log p_o(r,\gamma)}{\log \gamma}, \tag{29}$$

in which $p_o(r,\gamma)$ denotes the outage probability with the transmitter side SNR γ and the target rate $r \log \gamma$. The outage probability of our scheme is derived from Eq. (23) by

$$p_o(r,\gamma) = \Pr\left\{\frac{1}{N+1}\sum_{m=1}^{N} C_n < r\log\gamma\right\}, \tag{30}$$

in which C_n is given by Eq. (24).

Assume that the channel gain $g_{a,b}$ is a random variable obeying an exponential distribution with parameter $\frac{1}{\bar{g}_{a,b}}$, in which $\bar{g}_{a,b}$ denotes the average channel gain between nodes a and b. To better illustrate the DMT of this successive relaying protocol, we define v as a random variable determined by $\frac{1}{g_{a,b}}$. Based on [32], the relationship between v and $g_{a,b}$ can be given by

$$v = -\frac{\log g_{a,b}}{\log\gamma}. \tag{31}$$

The probability density function (p.d.f.) of v is given by

$$p(v) = \frac{1}{\bar{g}_{a,b}} \exp\left(-\frac{\gamma^{-v}}{\bar{g}_{a,b}}\right)\gamma^{-v}\ln\gamma. \tag{32}$$

In the high SNR regime, we have

$$\lim_{\gamma\to\infty} p(v) = \begin{cases} 0 & v < 0 \\ \dfrac{\ln\gamma}{\bar{g}_{a,b}}\gamma^{-v} & v \geq 0. \end{cases} \tag{33}$$

Specifically, we use v_n, u_n, $s_{m,n}$, and t_n to denote the variables of $\frac{1}{g_{S,n}}$, $\frac{1}{g_{n,D}}$, $\frac{1}{g_{m,n}}$, and $\tau_n = \frac{I_n+\sigma^2}{\sigma^2}$, respectively. Based on the above definition, we present the DMT of this successive relaying protocol in the following lemma.

Lemma 1: The DMT of this successive relaying protocol is obtained by

$$d(r) = \min_{O^+}\left\{\sum_{n=1}^{N}(v_n + u_n) + \sum_{m<n} s_{m,n}\right\}, \tag{34}$$

in which O^+ is the set of $(v_n, u_n, s_{m,n})$, i.e.,

$$O^+ = \left\{(v_n, u_n, s_{m,n}) \in \mathbb{R}^{3+}, (m, n = 1, 2, \cdots, N)\right|$$

$$\times \sum_{n=1}^{N}(1-\max\{t_n+v_n,u_n\})^+ < (N+1)r\Bigg\}. \quad (35)$$

Proof: The main idea of the proof is to obtain the outage probability of our scheme in the high SNR regime. By substituting $g_{a,b}=\gamma^{-v}$ into Eq. (30), the outage probability is written as

$$\begin{aligned}
&\lim_{\gamma\to\infty} p_o(r,\gamma)\\
&=\lim_{\gamma\to\infty}\Pr\left\{\sum_{n=1}^{N}\log\gamma^{\min\{1-v_n-t_n,1-u_n\}} < \log\gamma^{(N+1)r}\right\}\\
&=\lim_{\gamma\to\infty}\Pr\left\{\sum_{n=1}^{N}(1-\max\{v_n+t_n,u_n\})^+ < (N+1)r\right\}\\
&=\lim_{\gamma\to\infty}\int_{\sum_{n=1}^{N}(1-\max\{v_n+t_n,u_n\})^+<(N+1)r} p(\widetilde{v},\widetilde{u},\widetilde{s})d\widetilde{v}d\widetilde{u}d\widetilde{s}\\
&\overset{(a)}{\doteq}\lim_{\gamma\to\infty}\gamma^{-\min\limits_{O^+}\left\{\sum_{n=1}^{N}(v_n+u_n)+\sum_{m<n}s_{m,n}\right\}}, \quad (36)
\end{aligned}$$

in which O^+ is given by Eq. (35). The simplification in (a) in Eq. (36) is in a manner similar to the appendix in [32]. From Eqs. (29) and (36), it is seen that both the numerator and denominator in Eq. (29) approach to infinity with the same order. Therefore, we can get Eqs. (34) and (35), which establishes Lemma 1. ∎

To find the solution to the optimization problem in Eqs. (34) and (35), we further simplify this problem in the following lemma.

Lemma 2: The DMT of this successive relaying protocol can be obtained by the solution to the following optimization problem:

$$\begin{aligned}
d(r)=\ \min\quad & \sum_{n=1}^{N} v_n, && (37)\\
\text{s.t.}\quad & v_n\geq 0, && (38)\\
& \sum_{n=1}^{N}(1-nv_n)^+ \leq (N+1)r. && (39)
\end{aligned}$$

Proof: See Appendix C. ∎

Based on Lemma 2, we present the DMT of our scheme under the arbitrary relay ordering in the following theorem.

Theorem 5: The DMT of this successive relaying protocol with the arbitrary relay ordering is obtained by

$$d^*(r)=1-\frac{(N+1)r}{l}+\sum_{n=l+1}^{N}\frac{1}{n}, l-1\leq(N+1)r\leq l, \quad (40)$$

in which $l=1,2,\ldots,N$.

Proof: Our proof starts with the observation that the left side of Eq. (39) is a first-order polynomial of $\{v_n\}_{n=1}^{N}$. Therefore, the v_n with the larger coefficients should be selected to minimize $\sum_{n=1}^{N}v_n$ under the constraint of Eq. (39). When $l-1\leq(N+1)r\leq l, l=1,2,\ldots,N$, the first $(l-1)$ v_n shall take the minimum under the constraint of Eq. (38), i.e., $v_1=v_2=\cdots=v_{l-1}=0$. Thus, we get $\sum_{n=1}^{l-1}(1-nv_n)^+=l-1$. Based on the constraint of Eq. (39), we make $v_n\geq\frac{1}{n}, n=l+1,\ldots,N$. As a result, we have $(l-1)+(1-lv_l)\leq(N+1)r$, i.e., $v_l\geq 1-\frac{(N+1)r}{l}$. In particular, v^* that minimizes $\sum_{n=1}^{N}v_n$ is obtained by

$$\begin{aligned}
v_n^*&=0, \quad n=1,2,\ldots,l-1, && (41)\\
v_l^*&=1-\frac{(N+1)r}{l}, && (42)\\
v_n^*&=\frac{1}{n}, \quad n=l+1,\ldots,N. && (43)
\end{aligned}$$

Thus, we get $\sum_{n=1}^{N}v_n^*=1-\frac{(N+1)r}{l}+\sum_{n=l+1}^{N}\frac{1}{n}$, which completes the proof. ∎

D. POWER ALLOCATION

In the above discussion, the relay nodes and node S both transmit with a fixed power P. In this part, we discuss the power allocation scheme for this successive relaying protocol. Specifically, the node S is assumed to transmit in a fixed power P. We allocate the power among the relay nodes given a total power constraint. However, it is not trivial to obtain a feasible power allocation scheme in arbitrary transmission SNR. We present the asymptotic result of the power allocation among relay nodes in the high SNR regime.

Let P_n denote the power allocated to relay node n, i.e., $P_n=E\{|X_n[n+1]|^2\}$. The channel capacity C_n with power allocation is obtained by

$$C_n=\log\left(1+\min\left\{\frac{g_{S,n}P}{I_n+\sigma^2},\frac{g_{n,D}P_n}{\sigma^2}\right\}\right). \quad (44)$$

It is observed that the optimal power allocation must satisfy $P_n\leq\frac{g_{S,n}\sigma^2}{g_{n,D}(I_n+\sigma^2)}P$. Otherwise, the power allocated to relay n will be wasted. Assume that the total power constraint for the relay nodes is NP, i.e. $\sum_{n=1}^{N}P_n\leq NP$. Accordingly, we formulate the following power allocation problem:

$$\begin{aligned}
&\max_{\{P_n\}}\quad \frac{1}{N+1}\sum_{n=1}^{N}\log(1+\frac{g_{n,D}P_n}{\sigma^2})\\
&\text{s.t.}\quad \begin{cases}\sum_{n=1}^{N}P_n\leq NP\\ P_n\leq\frac{g_{S,n}\sigma^2}{g_{n,D}(I_n+\sigma^2)}P\\ P_n\geq 0.\end{cases} \quad (45)
\end{aligned}$$

To find the solution to problem (45) in the high SNR regime, we consider the case in which P and P_n approach infinity with equal order. We present the asymptotic result of the power allocation at relay node n when P and P_n approach infinity with equal order in the following theorem.

Corollary 1: When P approaches infinity, the optimal power allocated to relay n can be given by

$$P_n=c_nP, \quad (46)$$

where c_n is obtained through the following iterative equation:

$$c_n = \min\left\{\frac{g_{S,n}}{g_{n,D}\left(\sum_{j=1}^{n-1}\frac{\prod_{k=j}^{n-1} g_{k,n}c_k}{g_{S,n}^{n-j}}+1\right)}, 1\right\}. \quad (47)$$

In particular, $c_1 = \min\left\{\frac{g_{S,n}}{g_{n,D}}, 1\right\}$.

Proof: The main idea of this proof is based on "Water Filling in Cellar" policy [1], [33]. On the one hand, we use λ to denote the solution to $\sum_{n=1}^{N}\left(\lambda - \frac{\sigma^2}{g_{n,D}}\right)^+ = NP$. When the power is high enough, it can be seen that all relays will be allocated power. Accordingly, we derive

$$\lambda = P + \frac{1}{N}\sum_{n=1}^{N}\frac{\sigma^2}{g_{n,D}}. \quad (48)$$

Then, we have

$$P_n = P + \frac{1}{N}\sum_{n=1}^{N}\frac{\sigma^2}{g_{n,D}} - \frac{\sigma^2}{g_{n,D}}. \quad (49)$$

On the other hand, when P and P_n approach infinity with equal order, the minimum power of residual interference I_n is asymptotically obtained from Eq. (18) by

$$\lim_{P,P_1,\ldots,P_{n-1}\to\infty} I_n(P, P_1, \ldots, P_{n-1}) = \sigma^2\sum_{j=1}^{n-1}\frac{\prod_{k=j}^{n-1} g_{k,n}c_k}{g_{S,n}^{n-j}}. \quad (50)$$

Thus, it is obtained that

$$P_n = \frac{g_{S,n}}{g_{n,D}\left(\sum_{j=1}^{n-1}\frac{\prod_{k=j}^{n-1} g_{k,n}c_k}{g_{S,n}^{n-j}}+1\right)}P. \quad (51)$$

By referring to Eq. (27) in [1], the optimal power allocated to relay n is given by

$$P_n = \min\left\{\left(\frac{g_{S,n}}{g_{n,D}\left(\sum_{j=1}^{n-1}\frac{\prod_{k=j}^{n-1} g_{k,n}c_k}{g_{S,n}^{n-j}}+1\right)}P, \times P + \frac{1}{N}\sum_{n=1}^{N}\frac{\sigma^2}{g_{n,D}} - \frac{\sigma^2}{g_{n,D}}\right)\right\}. \quad (52)$$

Finally, we obtain the asymptotic expression of P_n in the high SNR regime by Eq. (46) and (47), which completes the proof. ■

V. NUMERICAL RESULTS

In this section, numerical results are shown to validate the theoretical analysis and further demonstrate the potential of our scheme. Assume that there are three DF relays in the cooperative communication system. We consider two cases of independent and identically distributed (*i.i.d.*) and independent non-identically distributed (*i.ni.d.*) Rayleigh fading channels. For *i.i.d.* case, we assume $\frac{1}{g_{a,b}} = 1$ for each node pair (a, b). For *i.ni.d.* case, we assume $\frac{1}{g_{a,b}} = d_{a,b}^{-2}$ in

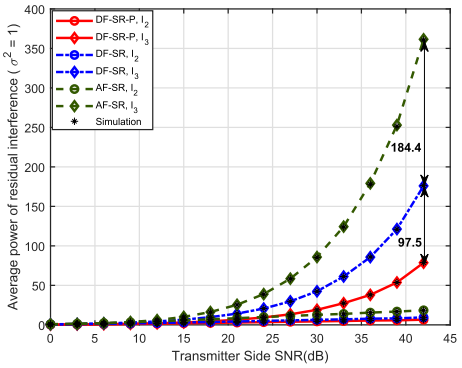

FIGURE 5. Simulation results and theory value of average minimum residual interference power.

which $d_{a,b}$ denotes the distance between node a and node b, due to the path-loss model. We consider the following network topology to determine $d_{a,b}$. Node S and node D are located in coordinates (0, 0) and (0, 1), respectively. The coordinates of three relays are given by $(\frac{\sqrt{3}}{2}, \frac{1}{2})$, $(-\frac{\sqrt{3}}{2}, \frac{1}{2})$, and $(0, \frac{1}{2})$, respectively. We first present the simulation result of the average minimum power of residual interference in *i.i.d.* case. Then we show the numerical results of average throughput and outage probability of this successive relaying protocol. To give more insights, our scheme is compared with two-timeslot DF relaying [10] and successive AF relaying [2]. For better illustration, we use "optimal" and "arbitrary" to denote the optimal relay ordering and arbitrary relay ordering, respectively. Let "DF-SR-P" and "DF-SR" stand for the proposed successive DF relaying protocols with equal power allocation and with the proposed power allocation scheme, respectively. Notations "DF-OR" and "AF-SR" refer to two-timeslot DF relaying [10] and successive AF relaying [2], respectively.

In Fig. 5, we present the average minimum power of residual interference versus transmitter side SNR curves. The theoretical minimum power of residual interference of DF-SR is obtained at arbitrary SNR by Eq. (18). It is observed that the simulation results of the average minimum power of residual interference match well with the theoretical values obtained by Eq. (18). As can be seen in Fig. 5, the average minimum residual interference power grows up as the transmitter side SNR increases. This is due to that the minimum residual interference power is determined by the channel coefficients in the high SNR regime from Eq. (19). The average minimum power of residual interference mainly depends on the cases in which one or more channel gains of the source-relay links are very low. Additionally, the proposed power allocation scheme can significantly further reduce the average minimum power of residual interference. In Fig. 6, we change the vertical coordinates into average $\log \tau_n$ to mitigate the impacts of those cases in which one or more channel gains of the source-relay links are very low. The gaps between DF-SR-P and DF-SR at the second and third relay nodes are 0.33 and 0.91, respectively. We next turn our attention to the comparison of DF-SR-P, DF-SR, and AF-SR. As shown in Fig. 6, both

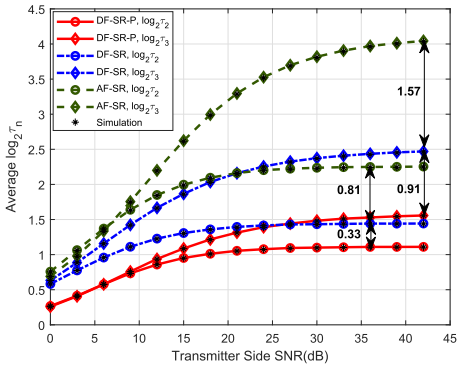

FIGURE 6. Simulation results and theory values of $\log \tau_n$, where $\tau_n = \frac{I_n+\sigma^2}{\sigma^2}$.

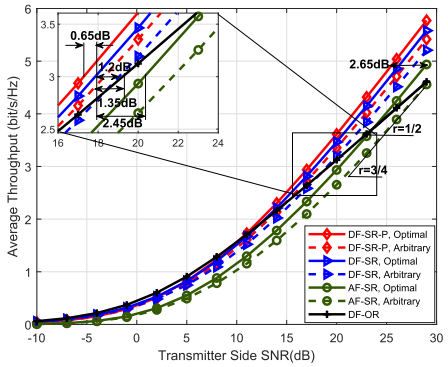

FIGURE 7. The Average Capacity of our scheme, two-timeslot DF relaying [10], and successive AF relaying [2] in $i.i.d.$ case.

DF-SR-P and DF-SR can reduce more power of residual interference in most cases. The gaps between DF-SR-P and AF-SR at the second and third relay nodes are 1.14 and 2.48, respectively. Moreover, in the high SNR regime, the average $\log \tau_n$ versus transmitter side SNR curves are smooth. This implies that the minimum residual interference power is bounded in the high SNR regime, which validates Theorem 3.

Fig. 7 and Fig. 8 show the average throughput versus transmitter side SNR curves in $i.i.d.$ and $i.ni.d.$ cases, respectively. The theoretical average throughput of DF-SR is obtained by Eq. (23) and (24). From the slopes of average throughput curves in the high SNR regime, the multiplexing gains of DF-SR-P and DF-SR are recovered to $\frac{3}{4}$. It is noted that different power allocation schemes and different relay orderings do not change the multiplexing gain. As can be seen in Figs. 7 and 8, the proposed power allocation scheme and the optimal relay ordering achieve the higher average throughput than equal power allocation and arbitrary relay ordering, respectively, in both $i.i.d.$ and $i.ni.d.$ cases. To achieve average throughput of 3 bit/s/Hz, DF-SR-P has SNR gains of 0.65dB and 0.3dB over DF-SR under the optimal relay ordering in $i.i.d.$ and $i.ni.d.$ cases, respectively. DF-SR with the optimal relay ordering has SNR gains of 1.2dB and 0.7dB over DF-SR with the arbitrary relay ordering in $i.i.d.$ and $i.ni.d.$ cases, respectively.

Next, we turn our attention to the comparison of DF-SR-P, DF-SR, DF-OR, and AF-SR. The multiplexing gain of

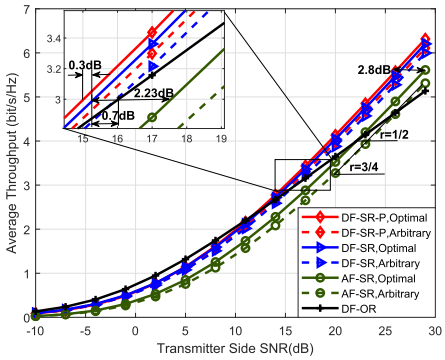

FIGURE 8. The Average Capacity of our scheme, two-timeslot DF relaying [10], and successive AF relaying [2] in $i.ni.d.$ case.

DF-OR is $1/2$, much lower than that of DF-SR-P and DF-SR, since it takes two timeslots to transmit one message. In the low SNR regime, DF-OR achieves the higher average throughput than DF-SR-P and DF-OR, while in the high SNR regime, the average throughput of DF-SR-P and DF-SR surpass that of DF-OR. This is because the advantage of high multiplexing gain for DF-SR-P and DF-SR is brought out by the high transmitter SNR. As a successive relaying, the multiplexing gain of AF-SR is the same as that of DF-SR-P and DF-SR, which is $\frac{3}{4}$. In terms of the average throughput, DF-SR-P and DF-SR outperform AF-SR under the optimal or arbitrary relay ordering. This is because that DF-SR-P and DF-SR can reduce much residual interference power than AF-SR. To achieve average throughput of 3 bit/s/Hz, DF-SR has SNR gains of 2.45dB and 2.23dB over AF-SR under the optimal relay ordering in $i.i.d.$ and $i.ni.d.$ cases, respectively. DF-SR with the optimal relay ordering has SNR gains of 1.35dB and 0.7dB over DF-OR in $i.i.d.$ and $i.ni.d.$ cases, respectively.

Fig. 9 and Fig. 10 show the curves of the outage probability versus transmitter side SNR for $r = 0$ in $i.i.d.$ and $i.ni.d.$ cases, respectively. Given the multiplexing gain, the diversity gains can be estimated from the slopes of the outage probability versus transmitter side SNR curves. We can obtain the theoretical diversity gain of DF-SR with the arbitrary relay ordering via Eq. (40). Specifically, when $r = 0$, the theoretical diversity gain is 1.83. As can be seen in Figs. 9 and 10, the theoretical values are validated by the simulation results. It is observed that the proposed power allocation scheme and the optimal relay ordering can further improve the outage performance. Moreover, it is noted that DF-OR has the optimal outage performance in both $i.i.d.$ and $i.ni.d.$ cases. This means DF-OR achieves low target rate more easily than DF-SR-P, DF-SR, and AF-SR. Compared with AF-SR, both of DF-SR-P and DF-SR can achieve the lower outage probability under the optimal or arbitrary relay ordering.

Fig. 11 and Fig. 12 show the curves of the outage probability versus transmitter side SNR for $r = 0.48$ in $i.i.d.$ and $i.ni.d.$ cases, respectively. From Eq. (40), when $r = 0.48$, the theoretical diversity gain of DF-SR with the arbitrary

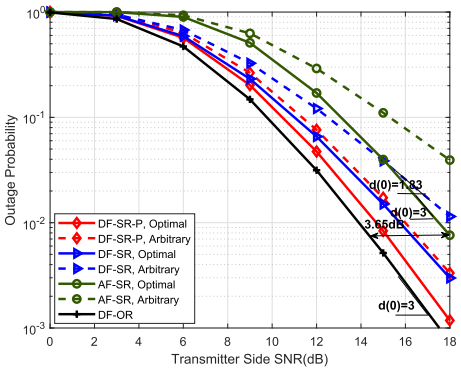

FIGURE 9. The Outage Probability of our scheme, two-timeslot DF relaying [10], and successive AF relaying [2] in $i.i.d.$ case. The target rate and multiplexing gains are set to be $R = 1$ and $r = 0$, respectively.

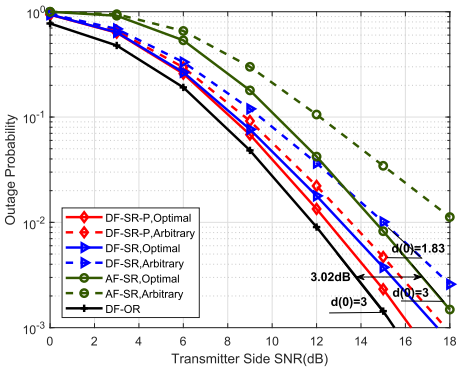

FIGURE 10. The Outage Probability of our scheme, two-timeslot DF relaying [10], and successive AF relaying [2] in $i.ni.d.$ case. The target rate and multiplexing gains are set to be $R = 1$ and $r = 0$, respectively.

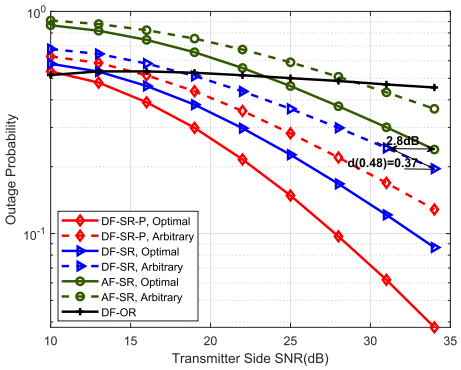

FIGURE 11. The Outage Probability of our scheme, two-timeslot DF relaying [10], and successive AF relaying [2] in $i.i.d.$ case. The target rate is set to be $R = r \log \gamma$, respectively.

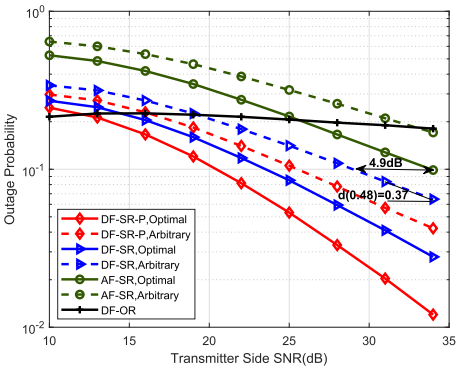

FIGURE 12. The Outage Probability of our scheme, two-timeslot DF relaying [10], and successive AF relaying [2] in $i.ni.d.$ case. The target rate is set to be $R = r \log \gamma$, respectively.

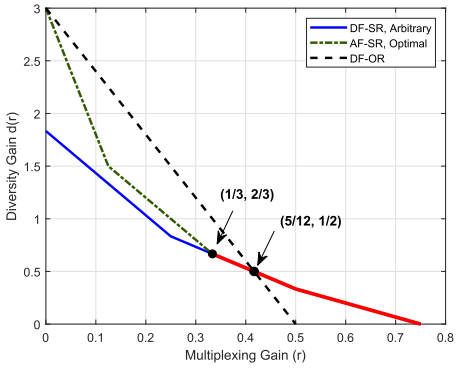

FIGURE 13. The Diversity Multiplexing Tradeoff, N = 3.

relay ordering is 0.37. As can be seen in Figs. 11 and 12, the simulation results validate the theoretical diversity gains in both $i.i.d.$ and $i.ni.d.$ cases. Additionally, both the proposed power allocation scheme and the optimal relay ordering can improve the outage performance of the proposed protocol. In case of $r = 0.48$, both DF-SR-P and DF-SR get notable diversity gains over DF-OR. It implies that DF-SR-P and DF-SR achieve high target rate more easily than DF-OR. This is because DF-SR-P and DF-SR can achieve the higher multiplexing gain than DF-OR. As Figs. 11 and 12 show, the outage performance of DF-SR-P and DF-SR outperforms that of AF-SR in both $i.i.d.$ and $i.ni.d.$ cases. Moreover, DF-SR with the arbitrary relay ordering achieves the same diversity gain with AF-SR with the optimal relay ordering. Specifically, DF-SR with the arbitrary relay ordering obtains SNR gains of 2.8dB and 4.9dB over AF-SR with the optimal relay ordering in $i.i.d.$ and $i.ni.d.$ cases, respectively.

Having validated the diversity gain given by Eq. (40) for sampling multiplexing gain $r = 0$ and $r = 0.48$, we next turn our attention to the comparison of DMT curves. As shown in Fig. 13, we draw the DMT curves of DF-SR with the arbitrary relay ordering, AF-SR with the optimal relay ordering, and DF-OR. It is seen that DF-OR has notable diversity gains over DF-SR with the arbitrary relay ordering when $r \in [0, 5/12]$, while the diversity gains of DF-SR with the arbitrary relay ordering exceed that of DF-OR when $r \in [5/12, 3/4]$, because DF-SR can achieve higher multiplexing gain as a successive relaying than DF-OR. Compared with AF-SR, DF-SR with the arbitrary relay ordering can achieve the same DMT as AF-SR with the optimal relay ordering in high multiplexing gain regime, i.e., $r \in [1/3, 3/4]$.

VI. CONCLUSION

In this paper, we have presented a successive relaying protocol that exploits multiple DF relay nodes. A privacy-aware

and low-complexity interference suppression method has been used to deal with the IRI caused by the concurrent transmission of the source and relays. Specifically, an interfered relay node actively keeps receiving signals from the source and uses these signals as prior knowledge to suppress IRI with a linear processing method. Since the relay node does not need to decode any signals intended for other relay and analog signal processing has been used to suppress the IRI, this protocol does not worry about the privacy disclosure and has the benefit of low complexity. We have derived the closed-form expression of the minimum power of residual interference. It is proved to be bounded even if the transmission power approaches infinity. Based on the boundedness of the minimum power of residual interference, we analyze the average throughput and DMT of this successive relaying protocol. Furthermore, we present a power allocation scheme in the high SNR regime for this successive relaying protocol. Both the theoretical analysis and simulation results have demonstrated the potential of our scheme. In terms of average throughput or outage probability, our scheme always outperforms successive AF relaying. As a successive relaying protocol, our scheme is capable of achieving higher multiplexing gain than conventional two-timeslot DF relaying.

APPENDIX A
PROOF OF THEOREM 1

The basic idea of the proof is to use the Lagrange Multiplier method. From Eqs. (9)-(14), the minimum residual interference power is rewritten as

$$I_n = \left|h_{n-1,n} - \boldsymbol{\omega}_n^{\intercal}\boldsymbol{\alpha}_{n,n-1}\right|^2 P + \sum_{j=1}^{n-2}\left|\boldsymbol{\omega}_n^{\intercal}\boldsymbol{\alpha}_{n,j}\right|^2 P + \sum_{j=1}^{n-1}\left|\boldsymbol{\omega}_n^{\intercal}\boldsymbol{e}_{n,j}\right|^2\sigma^2. \quad (53)$$

From the matrix differential calculus theory [36], we have $\frac{d^2 I_n}{d\boldsymbol{\omega}_n^2} = 2\mathbf{B}_n \succ 0$. Therefore, the optimal weight vector $\boldsymbol{\omega}_n$ that minimizes the power of residual interference I_n can be obtained by using the Lagrange Multiplier method. It is sufficient to show that I_n is minimized if and only if

$$\frac{dI_n}{d\boldsymbol{\omega}_n^{\intercal}} = 0. \quad (54)$$

From Eq. (53), it is derived that

$$\begin{aligned}\frac{dI_n}{d\boldsymbol{\omega}_n^{\intercal}} &= 2\left(\boldsymbol{\omega}_n^{\intercal}\boldsymbol{\alpha}_{n,n-1} - h_{n-1,n}\right)\boldsymbol{\alpha}_{n,n-1}^{\mathbf{H}} P \\ &= +2\sum_{j=1}^{n-2}\boldsymbol{\omega}_n^{\intercal}\boldsymbol{\alpha}_{n,j}\boldsymbol{\alpha}_{n,j}^{\mathbf{H}} P + 2\boldsymbol{\omega}_n^{\intercal}\mathbf{E}_{n-1}\sigma^2 \\ &= 2(\boldsymbol{\omega}_n^{\intercal}\mathbf{B}_n - h_{n-1,n}\boldsymbol{\alpha}_{n,n-1}^{\mathbf{H}} P), \end{aligned} \quad (55)$$

where $\mathbf{B}_n$ is given by Eq. (16). Substituting Eq. (55) into Eq. (54), we get $\boldsymbol{\omega}_n^{\intercal}\mathbf{B}_n = h_{n-1,n}\boldsymbol{\alpha}_{n,n-1}^{\mathbf{H}} P$. Moreover, the inverse of $\mathbf{B}_n$ is valid because it is a positive definite matrix. Therefore, the optimal weight vector $\boldsymbol{\omega}_n$ is obtained by Eq. (15), which proves Theorem 1.

APPENDIX B
PROOF OF LEMMA 1

The proof is based on the following observation. Based on Eq. (53), the minimum power of residual interference I_n is rewritten as

$$\begin{aligned} I_n &= g_{n-1,n}P - h_{n-1,n}\boldsymbol{\alpha}_{n,n-1}^{\mathbf{H}}\bar{\boldsymbol{\omega}}_n P - \bar{h}_{n-1,n}\boldsymbol{\omega}_n^{\intercal}\boldsymbol{\alpha}_{n,n-1}P \\ &\quad + \sum_{j=1}^{n-1}\boldsymbol{\omega}_n^{\intercal}\boldsymbol{\alpha}_{n,j}\boldsymbol{\alpha}_{n,j}^{\mathbf{H}}\bar{\boldsymbol{\omega}}_n P + \boldsymbol{\omega}_n^{\intercal}\mathbf{E}_{n-1}\bar{\boldsymbol{\omega}}_n\sigma^2 \\ &= g_{n-1,n}P - h_{n-1,n}\boldsymbol{\alpha}_{n,n-1}^{\mathbf{H}}\bar{\boldsymbol{\omega}}_n P - \bar{h}_{n-1,n}\boldsymbol{\omega}_n^{\intercal}\boldsymbol{\alpha}_{n,n-1}P \\ &\quad + \boldsymbol{\omega}_n^{\intercal}\left(\sum_{j=1}^{n-1}\boldsymbol{\alpha}_{n,j}\boldsymbol{\alpha}_{n,j}^{\mathbf{H}}P + \mathbf{E}_{n-1}\sigma^2\right)\bar{\boldsymbol{\omega}}_n \\ &\overset{(a)}{=} g_{n-1,n}P - h_{n-1,n}\boldsymbol{\alpha}_{n,n-1}^{\mathbf{H}}\bar{\boldsymbol{\omega}}_n P - \bar{h}_{n-1,n}\boldsymbol{\omega}_n^{\intercal}\boldsymbol{\alpha}_{n,n-1}P \\ &\quad + \boldsymbol{\omega}_n^{\intercal}\mathbf{B}_n\bar{\boldsymbol{\omega}}_n \\ &\overset{(b)}{=} g_{n-1,n}P - \bar{h}_{n-1,n}\boldsymbol{\omega}_n^{\intercal}\boldsymbol{\alpha}_{n,n-1}P, \end{aligned} \quad (56)$$

where $\bar{a}$ denotes the conjugate of a. In Eq. (56), the simplification in (a) follows from Eq. (16). The simplification in (b) follows from that $\boldsymbol{\omega}_n^{\intercal}\mathbf{B}_n\bar{\boldsymbol{\omega}}_n = h_{n-1,n}\boldsymbol{\alpha}_{n,n-1}^{\mathbf{H}}\bar{\boldsymbol{\omega}}_n P = \bar{h}_{n-1,n}\boldsymbol{\omega}_n^{\intercal}\boldsymbol{\alpha}_{n,n-1}P$. By substituting the optimal weight vector $\boldsymbol{\omega}_n$ in Eq. (15) into Eq. (56), we get $I_n = g_{n-1,n}P\left(1 - \boldsymbol{\alpha}_{n,n-1}^{\mathbf{H}}\mathbf{B}_n^{-1}\boldsymbol{\alpha}_{n,n-1}P\right)$. Since $\mathbf{B}_n$ is a function of P, Lemma 2 is established, which completes the proof.

APPENDIX C
PROOF OF LEMMA 3

Let us first show how to obtain t_n, in which $t_n = \frac{\log\tau_n}{\log\gamma}$, $\tau_n = \frac{I_n+\sigma^2}{\sigma^2}$. By substituting $g_{k,n} = \gamma^{-s_{k,n}}$ and $g_{S,n} = \gamma^{-v_n}$ into Eq.(20), it is obtained that

$$\lim_{\gamma\to\infty}\frac{\log\omega_n^2[j]}{\log\gamma} = (n-j)v_n - \sum_{k=j}^{n-1}s_{k,n}. \quad (57)$$

It is noted that $\lim_{\gamma\to\infty}\frac{\log\omega_n^2[j]}{\log\gamma} \geq 0$, and thus we have $(n-j)v_n \geq \sum_{k=j}^{n-1}s_{k,n}$. Based on Eq. (32), we have $v_n \geq 0$, $s_{k,n} \geq 0$. Therefore, we set $s_{k,n} = 0$ to achieve the minimum of $\sum_{n=1}^{N}(v_n + u_n) + \sum_{k<n}s_{k,n}$. From the above analysis, it is deduced that

$$\begin{aligned} t_n &= \lim_{\gamma\to\infty}\frac{\log(\sum_{j=1}^{n-1}\omega_n^2[j])}{\log\gamma} \\ &\overset{(1)}{=} (n-1)v_n. \end{aligned} \quad (58)$$

The step (1) in Eq. (58) follows from that when γ approaches infinity, the value of $(\sum_{j=1}^{n-1}\omega_n^2[j] + 1)$ is determined by the one that has the maximal exponential variable within $\{\omega_n^2[j]\}_{j=1}^{n-1}$.

Since we have $s_{k,n} = 0$ and $t_n = (n-1)v_n$, the optimization problem in Lemma 1 is simplified as

$$d(r) = \min \quad \sum_{n=1}^{N} (v_n + u_n) \tag{59}$$

$$\text{s.t.} \quad v_n \geq 0, u_n \geq 0 \tag{60}$$

$$\sum_{n=1}^{N} (1 - \max\{nv_n, u_n\}))^+ \leq (N+1)r. \tag{61}$$

From the left side of the Eq. (61), we observe that $v_n < u_n$ in the case of $nv_n = u_n$. Therefore, we let $u_n = 0$ to achieve the minimum of $\sum_{n=1}^{N} (v_n + u_n)$. Thus, the optimization problem (59) is further simplified to the Eq. (37), which completes the proof.

REFERENCES

[1] W. Chen, "CAO-SIR: Channel aware ordered successive relaying," *IEEE Trans. Wireless Commun.*, vol. 13, no. 12, pp. 6513–6527, Dec. 2014.

[2] S. Hu and W. Chen, "Successive Amplify-and-Forward relaying with network interference cancellation," *IEEE Trans. Wireless Commun.*, vol. 17, no. 10, pp. 6871–6886, Oct. 2018.

[3] K. B. Letaief, W. Chen, Y. Shi, J. Zhang, and Y.-J.-A. Zhang, "The roadmap to 6G: AI empowered wireless networks," *IEEE Commun. Mag.*, vol. 57, no. 8, pp. 84–90, Aug. 2019.

[4] P. Yang, Y. Xiao, M. Xiao, and S. Li, "6G wireless communications: Vision and potential techniques," *IEEE Netw.*, vol. 33, no. 4, pp. 70–75, Jul. 2019.

[5] A. Sendonaris, E. Erkip, and B. Aazhang, "User cooperation diversity-part I: System description," *IEEE Trans. Commun.*, vol. 51, no. 11, pp. 1927–1938, Nov. 2003.

[6] A. Sendonaris, E. Erkip, and B. Aazhang, "User cooperation diversity-part II: Implementation aspects and performance analysis," *IEEE Trans. Commun.*, vol. 51, no. 11, pp. 1939–1948, Nov. 2003.

[7] J. N. Laneman and G. W. Wornell, "Distributed space-time-coded protocols for exploiting cooperative diversity in wireless networks," *IEEE Trans. Inf. Theory*, vol. 49, no. 10, pp. 2415–2425, Oct. 2003.

[8] J. N. Laneman, D. N. C. Tse, and G. W. Wornell, "Cooperative diversity in wireless networks: Efficient protocols and outage behavior," *IEEE Trans. Inf. Theory*, vol. 50, no. 12, pp. 3062–3080, Dec. 2004.

[9] R. U. Nabar, H. Bolcskei, and F. W. Kneubuhler, "Fading relay channels: Performance limits and space-time signal design," *IEEE J. Sel. Areas Commun.*, vol. 22, no. 6, pp. 1099–1109, Aug. 2004.

[10] A. Bletsas, A. Khisti, D. P. Reed, and A. Lippman, "A simple cooperative diversity method based on network path selection," *IEEE J. Sel. Areas Commun.*, vol. 24, no. 3, pp. 659–672, Mar. 2006.

[11] C. Li, B. Xia, S. Shao, Z. Chen, and Y. Tang, "Multi-user scheduling of the full-duplex enabled two-way relay systems," *IEEE Trans. Wireless Commun.*, vol. 16, no. 2, pp. 1094–1106, Feb. 2017.

[12] H. Chen, G. Li, and J. Cai, "Spectral–energy efficiency tradeoff in full-duplex two-way relay networks," *IEEE Syst. J.*, vol. 12, no. 1, pp. 583–592, Mar. 2018.

[13] S. Yang and J.-C. Belfiore, "Towards the optimal Amplify-and-Forward cooperative diversity scheme," *IEEE Trans. Inf. Theory*, vol. 53, no. 9, pp. 3114–3126, Sep. 2007.

[14] Y. Fan, C. Wang, J. Thompson, and H. Poor, "Recovering multiplexing loss through successive relaying using repetition coding," *IEEE Trans. Wireless Commun.*, vol. 6, no. 12, pp. 4484–4493, Dec. 2007.

[15] H. Wicaksana, S. Ting, C. Ho, W. Chin, and Y. Guan, "AF two-path half duplex relaying with inter-relay self interference cancellation: Diversity analysis and its improvement," *IEEE Trans. Wireless Commun.*, vol. 8, no. 9, pp. 4720–4729, Sep. 2009.

[16] C. Luo, Y. Gong, and F. Zheng, "Full interference cancellation for two-path relay cooperative networks," *IEEE Trans. Veh. Technol.*, vol. 60, no. 1, pp. 343–347, Jan. 2011.

[17] Y. Ji, C. Han, A. Wang, and H. Shi, "Partial inter-relay interference cancellation in two path successive relay network," *IEEE Commun. Lett.*, vol. 18, no. 3, pp. 451–454, Mar. 2014.

[18] G. Dou, R. Deng, X. He, J. Gao, and Q. Wang, "Precoding-based inter-relay interference cancellation for Amplify-and-Forward two-path successive relay networks," *IEEE Signal Process. Lett.*, vol. 25, no. 2, pp. 229–233, Feb. 2018.

[19] C. Ren, H. Zhang, J. Wen, J. Chen, and C. Tellambura, "Successive two-way relaying for full-duplex users with generalized self-interference mitigation," *IEEE Trans. Wireless Commun.*, vol. 18, no. 1, pp. 63–76, Jan. 2019.

[20] R. Zhang, "On achievable rates of two-path successive relaying," *IEEE Trans. Commun.*, vol. 57, no. 10, pp. 2914–2917, Oct. 2009.

[21] H. Wicaksana, S. H. Ting, Y. L. Guan, and X.-G. Xia, "Decode-and-Forward two-path half-duplex relaying: Diversity-multiplexing tradeoff analysis," *IEEE Trans. Commun.*, vol. 59, no. 7, pp. 1985–1994, Jul. 2011.

[22] N. Nomikos and D. Vouyioukas, "A successive opportunistic relaying protocol with inter-relay interference mitigation," in *Proc. 8th Int. Wireless Commun. Mobile Comput. Conf. (IWCMC)*, Aug. 2012, pp. 228–233.

[23] Y. Hu, K. H. Li, and K. C. Teh, "An efficient successive relaying protocol for multiple-relay cooperative networks," *IEEE Trans. Wireless Commun.*, vol. 11, no. 5, pp. 1892–1899, May 2012.

[24] C. Zhai, L. Zheng, P. Lan, H. Chen, and H. Xu, "Decode-and-forward two-path successive relaying with wireless energy harvesting," in *Proc. IEEE Int. Conf. Commun. Workshops (ICC Workshops)*, Paris, France, May 2017, pp. 35–40.

[25] W. Chen, K. Letaief, and Z. Cao, "Network interference cancellation," *IEEE Trans. Wireless Commun.*, vol. 8, no. 12, pp. 5982–5999, Dec. 2009.

[26] X. He and A. Yener, "Cooperation with an untrusted relay: A secrecy perspective," *IEEE Trans. Inf. Theory*, vol. 56, no. 8, pp. 3807–3827, Aug. 2010.

[27] L. Dong, Z. Han, A. P. Petropulu, and H. V. Poor, "Improving wireless physical layer security via cooperating relays," *IEEE Trans. Signal Process.*, vol. 58, no. 3, pp. 1875–1888, Mar. 2010.

[28] C. Jeong, I.-M. Kim, and D. I. Kim, "Joint secure beamforming design at the source and the relay for an Amplify-and-Forward MIMO untrusted relay system," *IEEE Trans. Signal Process.*, vol. 60, no. 1, pp. 310–325, Jan. 2012.

[29] H. A. Shah and I. Koo, "A novel physical layer security scheme in OFDM-based cognitive radio networks," *IEEE Access*, vol. 6, pp. 29486–29498, 2018.

[30] R. H. Walden, "Analog-to-digital converter survey and analysis," *IEEE J. Sel. Areas Commun.*, vol. 17, no. 4, pp. 539–550, Apr. 1999.

[31] A. V. Oppenheim and R. W. Schafer, *Discrete-Time Signal Processing*. Englewood cliffs, NJ, USA: Prentice-Hall.

[32] L. Zheng and D. N. C. Tse, "Diversity and multiplexing: A fundamental tradeoff in multiple-antenna channels," *IEEE Trans. Inf. Theory*, vol. 49, no. 5, pp. 1073–1096, May 2003.

[33] W. Chen, P. Fan, and Z. Cao, "Water filling in cellar: The optimal power allocation policy with channel and buffer state information," in *Proc. IEEE Int. Conf. Commun. (ICC)*, May 2005, pp. 537–541.

[34] N. Nomikos, T. Charalambous, I. Krikidis, D. N. Skoutas, D. Vouyioukas, and M. Johansson, "A buffer-aided successive opportunistic relay selection scheme with power adaptation and inter-relay interference cancellation for cooperative diversity systems," *IEEE Trans. Commun.*, vol. 63, no. 5, pp. 1623–1634, May 2015.

[35] S. M. Kim and M. Bengtsson, "Virtual full-duplex buffer-aided relaying in the presence of inter-relay interference," *IEEE Trans. Wireless Commun.*, vol. 15, no. 4, pp. 2966–2980, Apr. 2016.

[36] J. R. Magnus and H. Neudecker, *Matrix Differential Calculus With Applications in Statistics and Econometrics*. Hoboken, NJ, USA: Wiley, 2007.

JIANJING WEI received the B.S. degree in electronic and information engineering from Yanshan University, Qinhuangdao, China, in 2018. She is currently pursuing the M.S. degree with the Department of Electronic Engineering, Beijing Jiaotong University. Her current research interests are in the areas of cooperative communication and signal processing.

JIE WEI received the B.E. degree in communication and information system from Jilin University, Jilin, China, in 2000, and the Ph.D. degree in information and communication engineering from Beihang University, Beijing, China, in 2006. Since 2009, she has been an Associate Professor with the School of Electronic and Information Engineering, Beijing Jiaotong University. She has authored more than 20 technical articles. Her broad research interests include speech enhancement, speech separation, and synthetic aperture radar image processing.

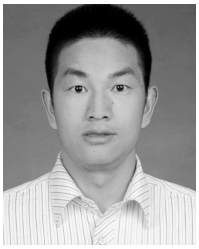

SHAOLING HU (Graduate Student Member, IEEE) received the B.S. and M.S. degrees in electronic and information engineering from the Harbin Institute of Technology, Harbin, China, in 2013 and 2015, respectively. He is currently pursuing the Ph.D. degree with the Department of Electronic Engineering, Tsinghua University. His research interests are in the areas of communications and networking.

WEI CHEN (Senior Member, IEEE) received the B.S. and Ph.D. degrees (Hons.) from Tsinghua University, in 2002 and 2007, respectively. From 2005 to 2007, he was a Visiting Ph.D. Student with The Hong Kong University of Science and Technology. Since 2007, he has been a Faculty Member with Tsinghua University. He visited the University of Southampton in 2010, Telecom Paris Tech in 2014, and Princeton University, Princeton, NJ, USA, in 2016. From 2014 to 2016, he was the Deputy Head of the Department of Electronic Engineering, Tsinghua University. He is currently a Tenured Full Professor, the Director of the Degree Office, and a University Council Member. He is also a Cheung Kong Young Scholar and a member of the National Program for Special Support of Eminent Professionals, also known as 10 000 Talent Program. His research interests are in the areas of communication theory, stochastic optimization, and statistical learning. Dr. Chen is a member of All-China Youth Federation. He received the IEEE Marconi Prize Paper Award in 2009 and the IEEE Comsoc Asia Pacific Board Best Young Researcher Award in 2011. He is a recipient of the National May 1st Labor Medal and the China Youth May 4th Medal. He has also been supported by the National 973 Youth Project, the NSFC Excellent Young Investigator Project, the New Century Talent Program of the Ministry of Education, and the Beijing Nova Program. He has served as a TPC Co-Chair for the IEEE VTC-Spring in 2011 and a Symposium Co-Chair for the IEEE ICC and Globecom. He serves as an Editor for the IEEE TRANSACTIONS ON COMMUNICATIONS.